




Review

Analysis of Pyrolysis Kinetic Parameters Based on Various Mathematical Models for More than Twenty Different Biomasses: A Review

José Juan Alvarado Flores ^{1,*}, Jorge Víctor Alcaraz Vera ², María Liliana Ávalos Rodríguez ³ , Luis Bernardo López Sosa ⁴ , José Guadalupe Rutiaga Quiñones ¹ , Luís Fernando Pintor Ibarra ¹, Francisco Márquez Montesino ⁵ and Roberto Aguado Zarraga ⁶

- ¹ Facultad de Ingeniería en Tecnología de la Madera, Universidad Michoacana de San Nicolás de Hidalgo, Edif. D. Cd. Universitaria, Av. Fco. J. Múgica s/n, Col. Felicitas del Rio, Morelia C.P. 58040, Michoacán, Mexico
- ² Instituto de Investigaciones Económicas y Empresariales, Universidad Michoacana de San Nicolás de Hidalgo, Cd. Universitaria, Av. Fco. J. Múgica s/n, Col. Felicitas del Rio, Morelia C.P. 58040, Michoacán, Mexico
- ³ Centro de Investigaciones en Geografía Ambiental, Universidad Nacional Autónoma de México, Antigua Carretera a Pátzcuaro No. 8701, Col. Ex Hacienda de San José de la Huerta, Morelia C.P. 58190, Michoacán, Mexico
- ⁴ Maestría en Ingeniería para la Sostenibilidad Energética, Universidad Intercultural Indígena de Michoacán, Carretera Pátzcuaro-Huecorio Km-3, Pátzcuaro C.P. 61614, Michoacán, Mexico
- ⁵ Departamento de Química, Universidad de Pinar del Rio, Pinar del Rio C.P. 20100, Cuba
- ⁶ Departamento de Ingeniería Química, Universidad Del País Vasco, UPV/EHU, P.O. Box 644, E48080 Bilbao, Spain
- * Correspondence: jjalvarado@umich.mx



Citation: Alvarado Flores, J.J.; Alcaraz Vera, J.V.; Ávalos Rodríguez, M.L.; López Sosa, L.B.; Rutiaga Quiñones, J.G.; Pintor Ibarra, L.F.; Márquez Montesino, F.; Aguado Zarraga, R. Analysis of Pyrolysis Kinetic Parameters Based on Various Mathematical Models for More than Twenty Different Biomasses: A Review. *Energies* **2022**, *15*, 6524. <https://doi.org/10.3390/en15186524>

Academic Editor: Francesco Frusteri

Received: 16 August 2022

Accepted: 4 September 2022

Published: 7 September 2022

Publisher's Note: MDPI stays neutral with regard to jurisdictional claims in published maps and institutional affiliations.



Copyright: © 2022 by the authors. Licensee MDPI, Basel, Switzerland. This article is an open access article distributed under the terms and conditions of the Creative Commons Attribution (CC BY) license (<https://creativecommons.org/licenses/by/4.0/>).

Abstract: Today, energy use is an important and urgent issue for economic development worldwide. It is expected that raw material in the form of biomass and lignocellulosic residues will become increasingly significant sources of sustainable energy in the future because they contain components such as cellulose, hemicellulose, lignin, and extractables with high energy-producing potential. It is then essential to determine the behavior of these materials during thermal degradation processes, such as pyrolysis (total or partial absence of air/oxygen). Pyrolyzed biomass and its residual fractions can be processed to produce important chemical products, such as hydrogen gas (H₂). Thermogravimetric (TGA) analysis and its derivative, DTG, are analytical techniques used to determine weight loss as a function of temperature or time and associate changes with certain degradation and mass conversion processes in order to evaluate kinetic properties. Applying kinetic methods (mathematical models) to degradation processes permits obtaining several useful parameters for predicting the behavior of biomass during pyrolysis. Current differential (Friedman) and integral (Flynn–Wall–Ozawa, Kissinger–Akahira–Sunose, Starink, Popescu) models vary in their range of heating speeds (β) and degree of advance (α), but some (e.g., Kissinger's) do not consider the behavior of α . This article analyzes the results of numerous kinetic studies using pyrolysis and based on thermogravimetric processes involving over 20 distinct biomasses. The main goal of those studies was to generate products with high added value, such as bio-char, methane, hydrogen, and biodiesel. This broad review identifies models and determines the potential of lignocellulosic materials for generating bioenergy cleanly and sustainably.

Keywords: TGA-DTG; kinetics of thermal processes; pyrolysis; thermodynamic analysis; kinetic models

1. Introduction

Today, tendencies in the production and exploitation of energies derived from renewable sources are spurring great interest in broadening total energy production and reducing dependence on fossil fuels [1,2]. The ongoing search for alternative sources using the

Earth's natural resources involves a broad scientific community whose goal is to achieve an energy transition based on bioenergy from natural materials that will reduce current harmful environmental impacts [3,4]. The need for sources of bioenergy to replace oil and its derivatives reflects the gradual, inevitable exhaustion of those sources and the serious environmental problems that come with global warming [5]. Hydrogen is deemed an excellent substitute for fossil fuels because its high heating value (HHV, 120 MJ/kg) is three times greater than that of gasoline [6] and because it can be obtained through the electrolysis of water, photolysis, and thermochemical processes using biomass, such as pyrolysis [7].

Residues of solid urban waste can generate as much as 20 MJ/kg of cellulose, a primary constituent of biomass [8]. Thermochemical conversion of lignocellulosic biomass is often a viable option for generating bioenergy and chemical products with added value [9,10]. The scientific literature reports a broad range of lignocellulosic materials (including agricultural, forest, and wood residues) that can be used to generate valuable energy resources. Because it is ecological and renewable, biomass is thought to have great potential for energy development [10,11]. Recent data show that bioenergy represents 17–36% of primary energy consumed worldwide, a clear indication of the importance of intensifying scientific research on organic materials that can be exploited as energy sources [12,13]. Each year, diverse countries, including Mexico, increase the energy they produce from renewable sources [2]. Mexico's current energy system is still based on fossil fuels (that supply 86.4% of primary energy), but renewable energies contribute 10.4% and biomass 5.2%, proportions that are similar to levels around the world [14,15]. Biomass, especially from lignocellulosic materials, has such great potential that it must continue to be explored and exploited. The eventual success of energy derived from these sources depends on technical innovation, social acceptance of the products obtained, and the type of biomass used [16]. The diverse types of biomasses have distinct molecular structures, chemical compositions, thermophysical properties, and potentials for hydrogen production [17]. Several processes, including thermal degradation, can be used to obtain a fuel such as biohydrogen from lignocellulosic materials, but these processes involve complex mechanisms and physical and chemical processes that demand detailed knowledge of the thermal and kinetic properties of chemical reactions since the heating rate, type of biomass, and atmosphere under which thermal degradation is conducted all significantly influence degradation speed and, hence, activation energy, that is, the amount of energy required to trigger those chemical reactions [18].

Thermogravimetric analysis (TGA) and its derivative, DTG, provide a guide to the viability, design, and optimization of bioenergy produced from biomass [19,20]. Unlike other approaches, such as calorimetry or Van Soest's method [21], which require more time and various special reagents, TGA analysis is fast and reliable. In studies of the effects of heating speed, temperature, and time on the development of thermal degradation reactions and the mechanisms involved in them, TGA analysis is commonly utilized to explore the degradation reactions of lignocellulosic materials and to quantify moisture, volatile matter, and the key kinetic parameters of thermal processes: activation energy (E_a), reaction order (n), and the pre-exponential factor (A) [19,22] that will influence future decisions on bioenergy production [23].

Diverse kinetic methods can be used to determine the parameters of lignocellulosic biomass, including the Friedman, Horowitz–Metzger, Van Krevelen, Coats–Redfern CR, Kissinger, Flynn–Wall–Ozawa (FWO), and Kissinger–Akahira–Sunose (KAS) models, all of which were designed to determine the best use of energy obtained from thermal processes, such as pyrolysis, the thermal conversion reaction that transforms biomass into gases and liquids of oxygenated organic compounds [24]. The biomass used can be as varied as cattle manure [25], incense sticks [26], cornstalks [27], pine waste [28], and microalgal-bacterial [29], among many other materials and residues. We review numerous studies of lignocellulosic materials and the application of various kinetic models that are required, for example, to ensure the total operativity of a biomass reactor.

2. Classification of Kinetic Models

Thermochemical processes applied to lignocellulosic biomass generate energy that can be exploited. Pyrolysis (total or partial absence of air/oxygen) uses an inert atmosphere (N₂, Ar, He) and specific operating conditions to produce liquid, solid (char), and gaseous (hydrogen) products. This thermal approach to processing biomass involves complex physical and chemical mechanisms that demand a complete understanding of the kinetic processes that occur during the reactions that take place. The basic kinetic parameters are E_a , n , and A . These can be calculated using various kinetic models of two main types: adjustment (statistical adjustment) and iso-conversional (free). Table 1 shows these models in relation to the point-slope equation.

Table 1. Mathematical models for the determination of kinetic parameters. [30].

$y = mx + b$					
Model	y	m	x	b	General Equation
¹ Friedman	$\ln\left(\frac{d\alpha}{dt}\right)$	$-\frac{E_a}{R}$	$\frac{1}{T}$	$\ln(A)$	$\ln\left(\frac{d\alpha}{dt}\right) = -\frac{E_a}{R} \times \frac{1}{T} + \ln(A)$
² FWO	$\ln(\beta)$	$-1.052 \frac{E_a}{R}$	$\frac{1}{T}$	$\ln\left(\frac{0.0048AEa}{R}\right)$	$\ln\beta = -1.052 \frac{E_a}{R} \times \frac{1}{T} + \ln\left(\frac{0.0048AEa}{R}\right)$
³ KAS	$\ln\left(\frac{\beta}{T^2}\right)$	$-\frac{E_a}{R}$	$\frac{1}{T}$	$\ln\left(\frac{AR}{E_a}\right)$	$\ln\left(\frac{\beta}{T^2}\right) = -\frac{E_a}{R} \times \frac{1}{T} + \ln\left(\frac{AR}{E_a}\right)$
⁴ Starink	$\ln\left(\frac{\beta}{T^{1.92}}\right)$	$-1.0008 \frac{E_a}{R}$	$\frac{1}{T}$	$\ln\left(\frac{0.732AEa}{R}\right)$	$\ln\left(\frac{\beta}{T^{1.92}}\right) = -1.0008 \frac{E_a}{R} \times \frac{1}{T} + \ln\left(\frac{0.732AEa}{R}\right)$
⁵ Popescu	$\ln\left(\frac{\beta}{T_n - T_m}\right)$	$-\frac{E_a}{R}$	$\frac{1}{T\zeta}$, $T\zeta = \frac{T_n + T_m}{2}$	$\ln\left(\frac{A}{F_{mn}}\right)$, $F_{mn} = \ln\left(\frac{1 - \alpha_m}{1 - \alpha_n}\right)$	$\ln\left(\frac{\beta}{T_n - T_m}\right) = -\frac{E_a}{R} \times \frac{1}{T\zeta} + \ln\left(\frac{A}{F_{mn}}\right)$
⁶ Kissinger	$\ln\left(\frac{\beta}{T^2}\right)$	$-\frac{E_a}{R}$	$\frac{1}{T_m}$	$\ln\left(\frac{AR}{E_a}\right)$	$\ln\left(\frac{\beta}{T^2}\right) = -\frac{E_a}{R} \times \frac{1}{T_m} + \ln\left(\frac{AR}{E_a}\right)$

¹ Differential model. ² FWO = Flynn–Wall–Ozawa (integral model). ³ KAS = Kissinger–Akahira–Sunose (integral model). ⁴ Starink = Integral model. ⁵ Popescu = Integral model. T_n = higher temperature, T_m = lower temperature. ⁶ Kissinger = Integral model. T_m = maximum weight loss peaks.

Iso-conversional models, such as Friedman, FWO, KAS, and Starink–Popescu, make it possible to predict the E_a as a function of the degree of mass conversion (α), independently of the multiple temperature programs utilized to obtain data on the heating speed (β) at a constant degree of conversion. Using these models, one can detect complex processes by analyzing the variation of E_a with respect to α [31].

3. Kinetics of Thermogravimetric Processes during Pyrolysis

3.1. Kinetics of Lignocellulosic Materials

Recent studies have applied thermogravimetric analysis (TGA) to *Sida cordifolia* L. biomass (Sida). The aim of that work was to characterize the thermal degradation of this biomass and evaluate its potential as an energy source using TGA carried out in a nitrogen/air atmosphere. Five heating speeds were used (10, 20, 30, 40, 50 °C min⁻¹) and the kinetic parameters were determined using the KAS and FWO models. Results showed that the average activation energies (E_a) determined by the two models in the inert atmosphere were 74.74 and 80.74 kJ mol⁻¹, respectively, while the values under combustion conditions were 51.08 and 58.91 kJ mol⁻¹. Together with the thermodynamic results (ΔH , ΔS , ΔG) and an HHV of up to 19 MJ/kg, results revealed *S. cordifolia* as a valuable raw material for producing bioenergy [32].

Agricultural residues have also been considered, with enormous potential for producing fuels, such as hydrogen. One reported the kinetics, thermodynamics, and physical characterization of corn collected in Wyoming, USA. The authors analyzed the kinetics and thermodynamics in detail using FWO and KAS, deriving E_a of 191.57 and 181.66 kJ/mol [33]. Biomass residues are important in countries such as India, which annually generates 14–23 million metric tons [34]. A recent study of corn there used TGA-

DTG to evaluate the kinetics of the pyrolysis of this biomass at three heating speeds (5, 10, 20 °C/min) in a nitrogen atmosphere ($N_2 = 99.99\%$, flow of 60 mL/min). Kinetic parameters were determined using the Friedman, FWO, KAS, and Starink iso-conversional models. Analysis of the thermal degradation graph (TGA) demonstrated that the greatest loss of mass occurred in a temperature range of 250–600 °C, indicating the best way to optimize the thermochemical conversion of this biomass. In this same range, DTG analysis revealed that the horizontal movement of the maximum temperatures of each of the three peaks along the “x” axis was due to a lower time of residence of the vapor in the biomass that reduced heat transference efficiency. Regarding kinetic behavior, slopes were observed with R^2 values between 0.951 and 0.999, so the E_a values of 186.06, 185.09, 197.63, and 185.80 kJ/mol were considered valid by the FWO, KAS, Friedman, and Starink models, respectively. Those values were also considered adequate for a thermochemical conversion process designed to produce energy.

In similarity to such a biomass residue, E_a values were practically equal in the FWO, KAS, and Starink models due to the mechanism of the equation applied in each one. One aim of that work was to reduce molecular interactions during pyrolysis, so the value of the A —which determines the level of molecular collision—was calculated at a low heating speed (5 °C/min) using the E_a value from the Friedman and KAS models. This parameter varied between 10^6 and 10^{23} , suggesting that the biomass was of complex composition, with high structural integrity. This phenomenon was also proven by the entropy behavior (ΔS), which flowed both negatively (−162.74 kJ/mol) and positively (189.80 kJ/mol). Gibbs free energy (ΔG) is calculated to determine the amount of energy present in a certain biomass. For the corncobs used in this study, it was determined that the approximate ΔG of 176 kJ/mol is greater than biomasses, such as *Typha latifolia*. All these results show that corncob residue is an excellent candidate for use as an energy source [35].

Dry leaves fallen from trees and discarded tires have also been considered in kinetics studies, as well as a mixture of both (dry leaves + tires) at a weight ratio of 1:1. Designing an efficient conversion unit requires precise data on the kinetics of pyrolytic reactions. Experiments with pyrolysis were carried out at four heating speeds (5, 10, 20, 40 °C/min) from 35–800 °C in a N_2 atmosphere using TGA. The TGA/DTG curves indicated that the three samples degraded principally in a broad temperature range of 350–450 °C, and that degradation increased at higher heating speeds. An elemental analysis showed that the mixture leaves + tires had a maximum HHV of 25.24 MJ/kg. To calculate this, two free methods—KAS and FWO—were applied to the TGA data. Results showed approximately equal (152 kJ/mol) average E_a of the raw material using these two methods, with a maximum error of 1.6%. Later, those E_a were inserted into the Coats–Redfern adjustment model to calculate the pre-exponential factors based on a first-order reaction speed. It is important to note that the amount of hydrogen reported in the elemental analysis of the leaves + tires mixture was 6.25% [36]. A different study of discarded tires determined an average E_a of 162.8 ± 23.2 kJ mol^{−1}, using the KAS and FWO methods and the Master Plot approach in a mass conversion range (a) of 0.20–0.80. In that case, hydrogen yield ($H_2 = 7.1\%$) was slightly higher than with the leaves + tires mixture [37].

Lentinula edodes pileus (LEP) and stipe (LES) fungi have been analyzed in kinetic studies to characterize the effects of four heating speeds (5, 10, 20, 40 K/min) in an air atmosphere using TGA and TG-FTIR. E_a was estimated using the distributed activation energy (DAEM), FWO, Starink, and Kissinger models. The average values obtained for the LEP fungus were 171.69, 181.12, 179.57, and 145.12 kJ/mol, respectively, while for LES they were 124.80, 133.60, 129.89, and 118.57 kJ/mol. Lower E_a values indicate that less energy is required to initiate a reaction due to weak links among the molecules in the sample. Therefore, the LES type showed great viability for joint combustion. Regardless of type, estimates of E_a were higher in the DAEM model than the other methods. Kissinger’s model generated the lowest E_a values due to its characteristics. The lower estimate of E_a by DAEM for LES compared to LEP signaled the lower temperature required to perform combustion. An ideal biofuel requires not only a low E_a but also parameters—HHV, for example—

to ensure that auto-thermal combustion is considered significant. That study reported hydrogen values of 6.43 and 6.7% for LEP and LES, respectively [38]. It is important to mention that an actualization of Kissinger's method, called Kissinger–Kai (K–K), has been used to conduct kinetic studies and calculate the E_a for primary components, as in the case of *Pinus sylvestris*, where hemicellulose and cellulose values of 155.99 and 156.94 kJ/mol were reported [39].

Work with several types of char (from Italy, South Africa, and Hungary) and biomass (stone pine and eucalyptus chips) presented kinetic characterizations based on TGA analysis and differential scanning calorimetry (DSC) with an evaluation of several combustion parameters. The FWO and KAS models were used for the kinetic analysis. E_a values for the stone pine and eucalyptus chips were high, above 370 and 420 kJ/mol, respectively. For the char, the E_a of the South African material was slightly above 170 kJ/mol. The elemental analysis found the largest amount of hydrogen (6.71%) in the pine chips [40].

Camel grass (*Cymbopogon schoenanthus*) has been another option in kinetic studies in an inert environment at three heating speeds (10, 30, 50 °C min⁻¹) to evaluate its bioenergy potential. Pyrolysis experiments were simultaneously conducted using a DSC, analyzer, and thermogravimetry. The thermal data for the kinetic parameters were analyzed by FWO and KAS. The values for the pre-exponential factors showed a tendency to follow first-order kinetics. The authors considered that given the amount of volatiles (82.67%), the high HHV (15 MJ kg⁻¹), low E_a (84–193 kJ/mol), and Gibbs free energy (173–177 kJ mol⁻¹) determined, this biomass has considerable potential for low-cost, direct conversion into gaseous fuels, such as hydrogen [41].

Agricultural biomass from peas was analyzed to determine its potential to produce bioenergy through pyrolysis. Experiments were carried out in a TG/DSC-FT-IR (4000–400 cm⁻¹) in an inert N₂ atmosphere at ambient temperatures as high as 800 °C, using four heating speeds (10, 20, 30, 40 °C/min). The kinetic parameters were calculated using the KAS, FWO, Starink, and Vyazovkin models. The analysis determined that E_a values increased proportionately to the degree of mass conversion (α) and were estimated in ranges of 184–313 kJ mol⁻¹, 184–307 kJ mol⁻¹, 184–313 kJ mol⁻¹, and 184–313 kJ mol⁻¹, with averages of 212.71, 211.55, 212.94, and 212.93 kJ mol⁻¹ by the KAS, FWO, Starink, and Vyazovkin models, respectively. The values for A (3.34×10^{16} – 1.23×10^{28} s⁻¹) indicated that the thermal process of that biomass was complex. It is important to mention that the variation in the ΔG (143.2–47.8 kJ/mol) was lower than for other terrestrial biomasses [11]. Another significant finding was the similarity of ΔH with E_a , as a difference of only 5 kJ/mol was reported. This promotes the generation of reactions in the thermal process. The compositional analysis showed up to 5.6% of hydrogen. Based on these results, using pea residue to produce bioenergy was judged feasible as long as it was mixed with some type of local biomass or char to achieve sustainability [42].

A type of fern characterized by abundance and fast growth –*Pteris vittate*– has also been analyzed in terms of combustion and emission efficiency. The E_a of its pseudo-components (hemicellulose, cellulose, lignin) were determined in relation to the main stages of degradation using four kinetic models: Friedman, FWO, Starink, and DAEM. Results of FWO showed E_a values for the first, second, and third stages of 188.6, 214.31, and 272.19 kJ/mol, respectively, with a correlation coefficient (R^2) greater than 0.9 throughout the range of thermal degradation. One especially significant finding was that the highest emission detected was for hydrogen, in the following relation: H₂ > NO > NO₂ > HCN > SO₂ [43].

A recent study examined the physicochemical and composition properties of residues of *Mesua ferrea* (Ceylon firewood), commonly called “palo fierro” due to the hardness of this wood. It has a tobacco brown color and is used to make beautiful sculptures. The material was evaluated by thermogravimetric techniques (TGA/DTG) and spectroscopy using three relatively low heating speeds (5, 10, 20 °C/min). The Friedman, KAS, FWO, and Tang models were applied in the kinetic study. The E_a values calculated were 259.0, 232.4, 230.4, and 232.6 kJ/mol, respectively. The value of A showed a variation of

1.74×10^{18} – $5.78 \times 10^{23} \text{ min}^{-1}$. The physicochemical analysis found average amounts of hydrogen, ash, and volatile material of 6.55, 1.6, and 77%, respectively [44].

A study of cotton stalks from the Maharashtra region of central India used TGA, pyrolysis, and gasification analyses to estimate the kinetic parameters of the thermal degradation process, including E_a . Five heating speeds were used (5–30 K/min) in pyrolysis in an inert N_2 medium at ambient temperatures up to 1073 K. Determination of the kinetic parameters was conducted with three models: KAS, FWO, and CR. Observations showed a variation of 100–120 kJ/mol for E_a , a n range of 3.9–4.8, and a A of 10^8 to $8 \times 10^8 \text{ min}^{-1}$. That study also utilized simple reaction kinetic (SRM) and distributed energy (DAEM) models, obtaining E_a values of 102 and 103 kJ/mol, n of 3.8 and 4, and pre-exponential factors of 8×10^8 and $5.4 \times 10^8 \text{ min}^{-1}$, respectively. The gasification process produced an average E_a of 214 kJ/mol, while the compositional analysis showed that the cotton stalks had as much as 6% hydrogen and an approximate HHV of 16 MJ/kg. The authors concluded that their results are useful for designing and optimizing a gasifier fueled by cotton stalks [45].

Bamboo is another kind of biomass that has recently drawn the attention of researchers in the field of the kinetics of thermogravimetric processes. For example, the energy potential of *Phyllostachys pubescens* from China has been studied with a focus on three parts of the tree: branches and leaves from the branches and stems. That experiment was conducted in an air atmosphere at four heating speeds (5, 10, 20, 40 °C/min) and from ambient temperature to 1000 °C. To estimate E_a the researchers utilized the FWO, KAS, and Friedman iso-conversional models with the CR method to determine the reaction model. In the calculations of E_a , FWO presented the best R^2 values, so that method defined the ranges for that parameter for the leaves from the branches (121.28–201.01 kJ/mol), the leaves from the stems (170.83–263.09 kJ/mol), and the branches (157.27–227.05 kJ/mol). Based on this reaction model, and in accordance with the CR method, a second-order model was defined, that is, where the function corresponded to the model $(1 - \alpha)^2$. An important result of approximately 17 MJ/kg was obtained for the HHV, indicative of a high combustion potential [46]. Regarding additional research related to bamboo, a study of the characteristics of the pyrolysis of Moso bamboo (*Phyllostachys pubescens*) obtained in Zhejiang province in China, analyzed the external, middle, and internal layers of the plant and the leaves, using TG-FT-IR and Py-GC/MS techniques (gas chromatography-pyrolysis/mass spectroscopy). Results showed that 70% of weight loss occurred in the stage of rapid pyrolysis at temperatures of 200–400 °C. The FWO model generated the following E_a values for the external, middle, and internal layers and leaves: 141.02–224.41, 137.85–160.69, 128.61–176.73, and 159.69–187.56 kJ/mol. The study reported that other important products derived from pyrolysis, including methane (CH_4), which can be used as a biofuel in solid oxide fuel cells (SOFC) [47].

A separate study compared the pyrolytic process of wood of the species *Fagus sylvatica* (European beech, a hardwood) and *Cunninghamia lanceolata* (Chinese fir, a softwood). The process required four heating speeds (5–60 K/min) in a range of 300–1000 K and a N_2 atmosphere with a flow of 100 mL/min. Two models were used to obtain the kinetic parameters: FWO and CR for E_a and the reaction mechanism, respectively. It is important to mention that the CR model was also used to determine E_a , but the value obtained was compared to that by FWO to select the most adequate reaction mechanism and to determine the A factor. For the hardwood, FWO showed a conversion range of $\alpha = 0.05$ – 0.85 and thermal degradation zones of the biomass, while E_a values varied from 151.89–173.95 kJ/mol throughout the degradation range. In the case of the softwood, values for this parameter varied from 182.19–193.50 kJ/mol. The correlation coefficients (R^2) for both biomasses remained above 0.90, though some values of 1.0 were obtained, for example, for the hardwood when $\alpha = 0.65$. For the softwood, the highest value for this parameter was 0.9995 at $\alpha = 0.85$. The elemental analysis of the two kinds of wood revealed the interesting observation that they share certain similarities, for example, hydrogen production of 6.34% for the hardwood and 6.46% for the softwood. Differences

were considered to reflect diverse aspects, including chemical composition, extractives, and anatomy [48].

Regarding the pyrolysis of black walnut wood, studies in an inert atmosphere (nitrogen) and with air utilized four heating speeds (5–40 K/min). The kinetic analysis of the thermogravimetric process was carried out with FWO and KAS to calculate E_a , which varied from 205–216 kJ/mol in the N_2 atmosphere. A variation below 1.1% was observed in both atmospheres. In air, E_a varied from 180–212 kJ/mol, leading to the conclusion that pyrolysis was achieved with greater facility in air because the reaction was exothermic. E_a values showed some variation in all stages of mass degradation. In the N_2 atmosphere, three stages were representative of the entire process. They were studied to obtain a reaction model using CR, which required analyzing 36 proposals to determine that model #21 ($[-\ln(1 - \alpha)]^3$) provided a very close approximation to the E_a obtained by FWO and KAS (205 kJ/mol) for stage 1. Similarly, for stage 2, the conclusion was that model #20 ($[-\ln(1 - \alpha)]^2$) generated an E_a value of 215 kJ/mol, which approached that obtained by FWO and KAS (216 kJ/mol). According to the proposed models, the growth mechanism in stages 1 and 2 was considered to be due to random nucleation. Stage three was dominated by a chemical reaction. The authors argued that pyrolysis in air also required reaction models 20 and 21 for stage 1, and models 20 and 6 ($[(1 - \alpha)]^{-3} - 1$) for stage 2 and stage 3, respectively. Finally, they calculated the average value of the natural logarithm of the A ($\ln A$) in N_2 (32.33 min^{-1}) and air (28.36 min^{-1}) [49].

In China, medicines derived from diverse weeds are well known for their curative properties—treating malaria, for example—though their low density is also important. A recent study examined the pyrolysis of the trunk and leaves of *Artemisia apiacea* (wormwood). The authors analyzed the thermal transformation kinetics of that species using KAS and FWO, considering 5 heating speeds (10–50 K min^{-1}) in a N_2 atmosphere with a heating range of 300–1000 K. The reaction mechanism of pyrolysis was analyzed by the CR mathematical model. As has been reported for other types of biomasses, lignin is more resistant to thermal degradation than the other two primary components (hemicellulose and cellulose). For the trunk of *A. apiacea*, calculations of E_a showed average values of up to 174.79 and 174.41 kJ/mol by FWO and KAS, respectively, with values for the leaves of 185.91 and 187.48 kJ/mol. These E_a values were calculated without considering the reaction mechanism. That operation required the CR method, which found that the models D2 $[(1 - \alpha)\ln(1 - \alpha) + \alpha]$ vs. $1/T$ and D4 $[1 - 2/3\alpha] - (1 - \alpha)^{2/3}$ vs. $1/T$, which corresponded to the integral form $G(\times)$ of the Valensi (2D) and Ginstling diffusions (3D), respectively, were responsible for pyrolysis. They further determined that the E_a values of 172.66 kJ/mol (D2) and 177.62 kJ/mol (D4) were similar to those calculated by FWO and KAS (174.79 and 174.41 kJ/mol) [50].

Thermal degradation of rice in an oxidative atmosphere was compared to biomass residues, such as pomace, plum pits, and peach and olive stones in a study that used three heating speeds (5–15 K min^{-1}) with Kissinger, FWO, DAEM, and CR kinetics models. Kissinger's model showed a variation in E_a of 52.75–116.92 kJ/mol for the devolatilization stage and 65.39–157.24 kJ/mol for the char combustion stage. Of these biomasses, pomace had the lowest E_a (52.75 kJ/mol), followed by plum pits (59.14 kJ/mol), peach stones (90.64 kJ/mol), and, finally, olive stones (116.92 kJ/mol). These results show that pomace is the best candidate for optimizing yield by combustion. The molecular fraction (A) that could react if E_a were equal to zero had variations of 1.21×10^4 – $7.96 \times 10^9 \text{ s}^{-1}$ (devolatilization) and 1.36×10^4 – $9.94 \times 10^{10} \text{ s}^{-1}$ (char combustion). For the FWO method, the values for E_a and A differed as the average values of the pomace, plum, peach, and olive biomasses for these parameters were 108.80 kJ/mol and $3.75 \times 10^{14} \text{ s}^{-1}$, 114.62 kJ/mol and $6.88 \times 10^6 \text{ s}^{-1}$, 83.04 kJ/mol and $3.29 \times 10^{11} \text{ s}^{-1}$, and 113.98 kJ/mol and $4.15 \times 10^{17} \text{ s}^{-1}$, respectively, in a conversion range of 0.1–0.7. Regarding E_a , results were very similar to those obtained using DAEM, though differences were seen in the pre-exponential factor. With respect to the non-iso-conversional methods, overall, the authors observed similarities in the results of the two models applied at all three heating velocities, as the averages

obtained were 80, 90, and 100 kJ/mol for 5, 10, and 15 K/min, respectively. Proportional to the heating speed, the A showed a variation of 10^9 – 10^{14} s⁻¹ for the devolatilization stage and 10^5 – 10^{13} s⁻¹ for the char combustion stage. The differences between these E_a and A values were due to the variables and the behavior assumed by each method [51].

We have mentioned the Friedman method in practically every study reviewed. Though this is a classic model for determining the kinetic parameters of thermal degradation processes, it has disadvantages, such as sensitivity to “noise” derived from the amount of TGA data. This led to the development of an alternative that modified this iso-conversional method with a numeric interpolation and then compared results to the KAS and FWO models. Wheat chaff and beech sawdust were the biomasses utilized in that experiment, which was conducted in nitrogen (50 mL/min) from 298–1023 K. The speeds used for the chaff and sawdust were 2.5, 5, 10, and 20 K/min, and 5, 10, and 20 K/min, respectively. Results showed that the modified Friedman model had greater precision and less background noise than KAS and FWO. For the straw, E_a varied from 154–176 kJ/mol for a range of $\alpha = 0.05$ – 0.60 and from 176–379 kJ/mol with $\alpha = 0.60$ – 0.85 . Figures for the sawdust showed variations of 155–220 kJ/mol ($\alpha = 0.05$ – 0.45) and 220–209 kJ/mol ($\alpha = 0.45$ – 0.70). At higher values for the degree of advance ($\alpha = 0.70$ – 0.85), E_a increased from 209 to 316 kJ/mol. The lines generated had R^2 values of 0.988 and 0.975, respectively, for the chaff and sawdust [52].

Sorghum, wheat, and rice bran are the three main components of a widely commercialized liquor in China, called *baijiu*. The fabrication of this drink generates enormous amounts of solid residues (*baijiu diuzao*) that, once the primary products have been utilized, can serve as a raw material for generating renewable energy. Some studies conducted to analyze the potential energy of this biomass by calculating its kinetic parameters applied the KAS and FWO models. The results of the latter permitted calculating other key parameters, such as the A and the three principal thermodynamic properties: ΔH , ΔG , and ΔS . For this purpose, the researchers utilized three heating speeds (10, 30, 50 K/min) in N₂ with a temperature range of 298–1273 K. The average E_a for the pyrolysis of *baijiu diuzao* was 150.98 and 152.86 kJ/mol by KAS and FWO, respectively. The authors mentioned that this biomass presented an E_a value lower than that of some marine biomasses, such as *Sargassum pallidum* and *Laminaria japonica*. The value of the A varied from 10^3 – 10^{13} s⁻¹, suggesting the presence of surface reactions and the formation of complex products. Significantly, this study also utilized the artificial neural network model, which produced the highest R^2 value (0.9999) and, therefore, was the best model for pyrolysis, with results even higher than those achieved by KAS ($R^2 = 0.98$ – 0.99) and FWO ($R^2 = 0.98$ – 0.99). Regarding the thermodynamic results, the value of ΔH presented almost the same value as E_a (difference of ~5 kJ/mol), which means that pyrolysis was favorable under those experimental conditions and that the formation of gaseous products is feasible. The average of 180 kJ/mol for Gibbs free energy is higher than biomasses, such as rice husk, demonstrating that *baijiu diuzao* may have more potential energy. The CR model determined that the reaction kinetics of the pyrolytic process followed a behavior that accords with three reaction orders present in zone two of DTG and that, moreover, were proportional to the concentration of reagents in a certain reaction model. The variables analyzed showed that *baijiu diuzao* biomass can be utilized to develop cleaner renewable energies [53].

3.2. Kinetics of the Shell-Peel of Lignocellulosic Biomass

Another case is argan tree bark (*Argania spinosa*), a by-product obtained during production of argan oil, which is used mainly in the cosmetics industry. This bark is considered an attractive source of cheap, renewable biomass for generating sustainable energy as one elemental analysis reported production of up to 6.32% of hydrogen. Its thermochemical conversion potential has been evaluated by TGA at four heating speeds (5, 10, 15, 20 °C min⁻¹), while its kinetic parameters in non-isothermal conditions have been calculated by FWO and KAS. Results showed that when the mass conversion level (α) fluctuated from 0.10 to 0.55, average E_a were 154 and 145 kJ/mol. However, a drastic reduction was

seen when $\alpha \geq 0.6$, indicative of the kinetic complexity of a combustion process characterized by a faster reaction due to an intense devolatilization stage. In general, results emphasized the potential of using argan bark as biomass for thermal conversion through combustion [54].

Recently, diverse bio-residues called ‘second-generation’ have been assessed for producing biofuels. A study in Colombia analyzed thousands of tons of agroindustrial by-product biomass from pineapples (741, 300 tons), oranges (238,100), mango peel (318, 628), and rice bran (2.1 million), and a large amount of pine wood gathered from an expanse of 330,000 hectares. Pineapple, orange, and mango residues made up 29–40% of the mass. The kinetics of the thermogravimetric process were studied to establish the potential energy of the residues of these five products and to determine their principal parameters, such as E_a . The study applied five iso-conversional or free type models (KAS, FWO, Starink, Vyazovkin, Friedman) and an adjustment model (DAEM). Tests were conducted at 5, 10, and 20 °C/min in an inert N₂ atmosphere at 150 mL/min and a temperature range of 25–800 °C. Results for the ranges of variation in E_a revealed that all the biomasses presented complex processes. The five iso-conversional models showed diverse behaviors for each biomass. For example, the pineapple residue maintained a variation of 120–250 kJ/mol. The behavior of the orange and mango residues was similar, with maximum values of 400 and 350 kJ/mol, respectively, and an approximate conversion value of 50%. The rice and pine wood residues generated very similar values of 170 and 180 kJ/mol, respectively, but with a broad conversion range (10–80%). Results of the DAEM adjustment model showed similar patterns, as the variation of E_a was 150–550 kJ/mol [55].

Rice is one of the cereals most consumed worldwide. Indeed, it is considered the third-most important product for human consumption, and the first in the countries of the Association of Southeast Asian Nations (ASEAN, Brunei, Cambodia, Indonesia, Laos, Malaysia, Myanmar, the Philippines, Singapore, Thailand, Vietnam). The ASEAN estimates that annual rice production for processing exceeds 130 million tons, which generates millions of tons of residue. This presents an enormous opportunity for generating clean energies. One option for using this by-product is to produce synthesis gas. One study explored applications of rice residues with various catalyzers: nickel, natural zeolite, and char ash. The rice chaff was obtained from a factory (BERNAS) in Malaysia. The kinetic studies used the Friedman, FWO, KAS, and CR models with heating speeds of 10, 20, 30, and 50 K/min. R^2 values were above 0.98. The average E_a values for Friedman’s model were 1.908×10^5 , 1.616×10^5 , 1.548×10^5 , and 1.614×10^5 J/mol, respectively, for the rice chaff with nickel, zeolite, and char ash. The E_a by FWO were 1.857×10^5 , 1.627×10^5 , 1.574×10^5 , and 1.614×10^5 J/mol, while the values for the KAS model were 1.839×10^5 , 1.629×10^5 , 1.553×10^5 , and 1.614×10^5 J/mol. Finally, CR obtained average E_a values of 60.15, 56.51, 51.35, and 53.56 kJ/mol for the four heating speeds and the catalyzers mixed with the rice chaff. As previously mentioned, the E_a calculated by the CR method is lower because of the degradation stages it considers. The lowest E_a were reported for the mixture with zeolite, in a range of 51.35–157.4 kJ/mol. The value of the A varied at orders of magnitude between 10^3 and 10^{17} [56].

In another recent study involving rice chaff, researchers attempted to improve catalysis in the pyrolytic process by adding rice chaff ash as a catalyzer. That study used four heating speeds (10–100 K/min) and the same kinetic methods (Kissinger, Friedman, KAS, FWO) to determine the parameters of E_a and A , and to compare the thermal process with and without the catalyzer. Results showed that adding the ash lowered the average E_a to 1.526×10^5 , 1.512×10^5 , and 1.536×10^5 J/mol according to the Friedman, KAS, and FWO models. Although Kissinger’s method considered only the value of the maximum peak (maximum temperature) of the DTG and did not include variability in the degree of advance of the reaction (α), results were very similar ($E_a = 1.463 \times 10^5$ J/mol) to those of the other three models. Overall, the Friedman, KAS, and FWO models showed greater reliability. It is important to note that value of the frequency factor also decreased by various orders of magnitude when ash was added as a catalyzer to

values of 10^{16} – 10^{13} min^{-1} . That study included a thermodynamic analysis of the enthalpy, entropy, and Gibbs free energy parameters. The latter ($\Delta G = 146$ – 189 kJ/mol) showed that the biomass has great potential for producing bioenergy [57].

Recent studies in the province of Baluchistan, Pakistan have explored two types of char and diverse agricultural residues, including char from Chamalang, and Dukki, rice and corn chaff, the central part (disk) of sunflowers, and phalsa (*Grewia asiatica*). The experiment was performed with 0.5 g samples using four heating speeds ($\beta = 10, 20, 30, 40$ °C/min) in nitrogen (3.5 L/min). The maximum temperature was 950 °C. To compare the applicability of these biomasses, a kinetic analysis was conducted using two adjustment models (Arrhenius, CR) and two models without adjustment, the free or iso-conversional Friedman and Vyazovkin methods. Results for the latter showed that E_a varied from 22–38 kJ/mol, with the lowest and highest values for the rice chaff biomass (22.44 kJ/mol) and Chamalang char (37.59 kJ/mol), respectively, as determined by the CR and Arrhenius models. It is important to mention that R^2 values were relatively low, in some cases just 0.674 (Dukki char), while the highest value was 0.944 for the Chamalang char. Results for E_a by the Friedman and Vyazovkin models were practically equal. The value of E_a decreased in the order: Chamalang char > Dukki char > sunflower disks > rice chaff > phalsa > corn chaff. In this case, the R^2 value was above 0.95, so the conclusion was that the iso-conversional models are more appropriate for estimating the kinetic parameters of both char and agricultural residues [58].

As mentioned above, residues of agricultural crops include materials rich in hemicellulose, cellulose, and lignin. India is the largest banana-consuming country in the world at over 100 million tons annually. Hence, one of the most abundant sources of agricultural residues there is banana exploitation. In fact, reports indicate that for every ton of fruit produced, 100 kg are rejected. Those residues could generate 3 tons of pseudo-stems, 480 kg of leaves, 440 kg of peel, and 160 kg of stems [59], all with great potential for exploitation to produce energy. It is important then to conduct research to determine their behavior in thermal conditions and their kinetic and thermodynamic properties during pyrolysis. One such study was carried out in a nitrogen atmosphere (20 mL/min) at three heating speeds (10, 20, 30 °C/min) from ambient temperature to 900 °C. That procedure was used to determine the kinetic parameters (E_a , A) and R^2 using five models: KAS, FWO, Starink, Friedman, and Kissinger. For the first four models, the average E_a values obtained were 79.36, 84.02, 92.12, and 73.89 kJ/mol, respectively. The value for Kissinger's model was 70.75 kJ/mol. The authors observed that pyrolysis of banana leaves may be more efficient than of other parts of this biomass, such as stems, since those E_a values were above 155.41 kJ/mol by Friedman's method and above 108.42 kJ/mol by Kissinger's [60]. E_a increased in the conversion range from 0.1 to 0.7, indicating an endothermic process, but for values of $\alpha > 0.7$ behavior was exothermic. The A calculated by Kissinger's method showed a variation between 10^7 and 10^{33} . This means that the pyrolytic process of banana leaves was complex. In all the models applied, R^2 values were above 0.94. Regarding the thermodynamic parameters, calculated on the basis of the E_a from the FWO and KAS models, average values for enthalpy and Gibbs free energy were 81.33 and 64.39 kJ/mol and 76.67 and 64.48 kJ/mol. Enthalpy was positive ($\alpha = 0.1$ – 0.7) and indicative of endothermic behavior. However, Gibbs free energy increased in the conversion range from 0.1 to 0.5. With respect to entropy, both negative and positive values were observed, as this increased from 0.1 to 0.7, suggesting that the thermal process was spontaneous and proportional to the temperature increase [61].

3.3. Kinetics of Products Derived from Cellulose

One of the most important derivatives of cellulose is nitrocellulose which, among other applications, is used to elaborate explosives. In general, nitrate content and aging are the main reasons for analyzing this material by TGA, including its thermal transformation kinetics. Kissinger's model was used to determine the kinetic parameters of nitrocellulose in an air atmosphere at a flow of 50 mL/min. The kinetic parameters calculated

were E_a and the natural logarithm of the pre-exponential factor. E_a values varied from 230.2 kJ mol⁻¹ (at 24 days of aging) to 310.5 kJ mol⁻¹ (at 72 days), while the natural logarithm of the A varied from 8 s⁻¹ (at 24 days) to 13 s⁻¹ (at 72 days). Due to the nature of Kissinger's model, which does not show optimal exactitude in the parameters calculated compared to other studies of nitrocellulose, the conclusion reached was that another model—such as KAS—could be applied to improve exactitude. Finally, the study found that nitrocellulose reached its greatest stability at 32 days of aging [62].

Similar to that study, other works have presented the results of kinetic studies of nitrocellulose derived from fibers and splinters of biomass. The heating speeds were 5, 10, 15, and 20 °C with a heating ramp of 30–300 °C. None of the models applied in that experiment (free, KAS, FWO, Friedman, Tang et al., DAEM) considered the reaction mechanisms. KAS, FWO, Tang et al., and DAEM produced similar average values (~95 kJ/mol). Friedman's model found one of the highest E_a values, attributable to the characteristics of that method—which calculates approximations—and the fact that none use a reaction model [63].

The thermal degradation of nitrocellulose has also been studied using the plasticizer dibutyl phosphate (C₁₆H₂₂O₄). That thermal degradation study determined E_a , calculated by the KAS, FWO, and Friedman models. Four heating speeds (5, 10, 15, 20 °C/min) were used in a nitrogen atmosphere at a constant flow of up to 50 mL/min. The degree of advance showed a variation of 0.1–0.9 with a step of 0.1. Results showed average E_a values of 117.4, 119.4, and 133.0 kJ/kg, respectively, for the three models. The first two values are almost equal, but due to discrepancies derived from the algorithm, a difference of over 10 kJ/kg existed with the Friedman method. The authors affirmed that the E_a values can be considered precise because R^2 was above 0.94. They concluded that nitrocellulose is stable at an average temperature of 200 °C [64].

3.4. Kinetics of Other Potentially Important Biomasses

Current research includes biomasses with potential energy that do not necessarily have high lignin content, including invasive weeds, such as canary grass (*Phalaris arundinacea*) of the family of the *Poaceae*. A kinetic study of this biomass evaluated its energy performance by applying the FWO, Starink, KAS, CR, and Vyazovkin models to determine the compensation effect (pre-exponential factor). The temperature range was 25–800 °C and four heating speeds were used (10–40 °C/min) in an inert nitrogen atmosphere (50 mL/min) for each sample of biomass (9.5 mg). The average E_a values calculated by the FWO, KAS, and Starink models were 161.29, 159.61, and 160.14 kJ/mol, respectively. A values varied from 10⁴ to 10¹³ s⁻¹ for those models. The CR method determined that the reaction model corresponded to a global reaction mechanism, on the order of F5. The additional Fourier transform infrared (FT-IR), gas chromatography, and mass spectroscopy analyses demonstrated that this weed is an optimal candidate for bioenergy production [65].

Palm oil is one of the most important oils in the world. Malaysia is a leading country in palm oil production. Today, this oil is produced on a surface of over 5,400,000 hectares and represents 90% of total biomass residues in the country. Seeking to determine the potential energy of such an enormous amount of residue, researchers have conducted experiments using the thermal process called slow pyrolysis, or torrefaction, which increases the properties of energy density, grindability, microbial resistance, and biodegradation. The raw material was palm leaves from Klang province (Selangor, Malaysia). Optimizing the thermochemical conditions of a torrefaction reactor requires calculating the best-known kinetic parameters (E_a , A , reaction mechanism) using an integral model (KAS) and an adjustment model (Coats–Redfern). Thermal degradation (TGA) during the torrefaction process was conducted from ambient temperature to 800 °C in a nitrogen atmosphere at a flow of 50 mL/min. The kinetic analysis was carried out at four heating speeds ($\beta = 5, 10, 15, 20$ °C/min), considering an advance range of 0.05 ($\alpha = 0.05$ –0.95). Results by the KAS method showed that E_a for the first stage of degradation (hemicellulose) varied from 250–268 kJ/mol ($\alpha = 0.05$ –0.50) and from 204–400 kJ/mol for the second stage (cel-

lulose) for the rest of the conversion degree ($\alpha = 0.55$ – 0.95). Observations of both stages showed an initial R^2 above 0.95, though by the end of the conversion process ($\alpha = 0.95$, $E_a = 403.68$ kJ/mol), the R^2 value of 0.75 was comparatively low. For the CR adjustment model, average E_a value was lower, at just 109.28 kJ/mol. As mentioned above, this difference reflects the fact that the KAS method does not consider the reaction mechanism, in contrast to the adjustment model, which requires a mass-dependent function. Results indicate that palm leaves have significant potential as a source of bioenergy [66].

The paper industry is a particularly important branch of a nation's economic development. Similar to the study just examined, India was the site of research that explored the potential energy of paper production residue (Yash Paper Limited, Faizabad, India). The raw material used there is sugarcane bagasse. In this study, the energy analysis was based on (i) residues from mechanical pulping and (ii) the effect of adding Montmorillonite clay (silicate) to the pyrolytic process. TGA analysis was performed with 6–8 mg samples at heating speeds of 20, 25, and 30 °C/min in a temperature range of 25–1000 °C. To determine the kinetic (E_a , A) and thermodynamic (ΔH , ΔG , ΔS) parameters, researchers used the FWO, DAEM, and Vyazovkin models. For the residues from the paper factory with no clay added, the average E_a values by these models were 174.30, 286.32, and 184.75 kJ/mol, respectively. The average behavior of A was 5.36×10^{20} , 5.71×10^{23} and 7.74×10^{22} s⁻¹, respectively, while the values for the thermodynamic properties varied in the following approximate ranges: 169–280 kJ/mol, 177–180 kJ/mol, and -1.64 – 165.85 kJ/mol, respectively, for ΔH , ΔG , and ΔS . In contrast, the average E_a values for the three models were 166.19, 257.20, and 173.25 kJ/mol for the residues with added Montmorillonite clay. The average values for A were 8.62×10^{19} , 2.50×10^{22} and 5.90×10^{21} s⁻¹. The values for the thermodynamic properties showed an approximate variation of 161–252 kJ/mol, 178–181 kJ/mol, and -21 – 117 kJ/mol, respectively, for ΔH , ΔG , and ΔS . These results showed that adding the clay reduced the E_a , enthalpy, and entropy values, though Gibbs free energy remained unchanged. The authors concluded that these results indicate the possibility to improve the yield of pyrolysis using sugarcane bagasse residue from paper production [67].

Another kind of residue that can be used conveniently to produce energy is solid municipal waste with residues from paper production. These residues usually contain food waste (46.4%), PVC (30.7%), waste wood (4.7%), and paper (18.2%). Some authors have studied the effects of pre-treatment with ultrasound followed by thermal degradation of these materials. Results showed E_a values of 201.545 kJ/mol for solid municipal residues (SMR) and 237.202 kJ/mol for paper manufacturing residues (PMR). Calculating this parameter required only the DAEM model since the R^2 value was above 0.99 for the entire thermal process. What stood out in the compositional analysis were high ash values of approximately 9.4 and 60% for SMR and PMR, respectively. Hence, volatile content was higher in the SMR residues ($>13,000$ kJ/mol), as was hydrogen content, at approximately 6% [68].

Two other kinds of biomass from India have also been studied: residues from the neem tree (*Azadirachta indica*) that is used mainly in Ayurveda medicine and medicine on the Indian sub-continent and Indian gooseberry (*Phyllanthus emblica*). Due to their high renewability, these are thought to generate biomass residues with high energy potential. Kinetic degradation studies have been conducted with these residues using pyrolysis and the KAS, Friedman, FWO, DAEM, Coats–Redfern, Vyazovkin, and Criado models with $\beta = 10, 20, 30, 40,$ and 50 °C/min in a nitrogen atmosphere. The average E_a values for *A. indica* by the KAS, FWO, Friedman, and DAEM models were 176.66, 193.67, 196.06, and 177.32 kJ/mol, and average values for *P. emblica* were 184.77, 195.10, 189.95, and 186.46 kJ/mol, respectively. The A was also calculated, showing a variation of various orders of magnitude (10^{13} – 10^{20} min⁻¹). The Coats–Redfern model was applied to determine the n of these two biomasses. The values reported were 1, 1.9, and 2.7 for both residues. For Vyazovkin's model, average E_a were 204.24 and 184.58 kJ/mol for *A. indica* and *P. emblica*. In this case, E_a increased proportionally to the degree of advance (α). The authors considered that the latter is the model most recommendable for these two kinds of biomass, followed

by Friedman, FWO, and DAEM, though CR (an integral model) obtained the lowest E_a . The thermodynamic parameters of the *A. indica* residues had average enthalpy values of 188.50, 190.90, and 199.07 kJ/mol, measured by FWO, Friedman, and Vyazovkin, respectively. Enthalpy values for *P. emblica* showed a variation of 189.93, 181.29, and 179.41 kJ/mol, using the same models. Clearly, these results are similar to the values determined for E_a . In addition, they show that this biomass requires greater energy for thermal degradation than *A. indica*. One particularly interesting aspect of this study involves the Gibbs free energy values, which reported an average of ~215 kJ/mol for both materials. Overall, results show that both biomasses have potential to generate bio-energy [69].

Currently, over 5 million tons of tea are produced worldwide [70]. An experimental study quantified the pyrolysis behavior of tea residues using four heating speeds with Fourier transform infrared spectrometry (FT-IR), thermogravimetry, gas chromatography, and mass spectrometry. The estimates of the average E_a for the three stages of thermal degradation were 161.81, 193.19, and 224.99 kJ/mol, respectively, using the FWO and KAS models. The amount of hydrogen produced according to the elemental analysis was 6.60%. A total of 33 organic compounds were identified, including alkene, acid, benzene, furane, ketone, phenol, nitride, alcohol, aldehyde, alkyl, and ester. That study provided theoretical and practical guidelines for dealing with the engineering challenges involved in introducing tea residues into the bioenergy sector [71].

3.4.1. Kinetics of Marine and/or Aquatic Biomass

In another study in Malaysia, samples of powdered biomass from a species of alga, *Chlorella vulgaris*, were subjected to pyrolysis to analyze kinetics and thermodynamic yields by means of TGA. The FWO, KAS, Starink, and Vyazovkin models (V) were used to evaluate the kinetic parameters. The study reported E_a values in the range of 156.16–158.10 kJ/mol, 145.26–147.84 kJ/mol, 138.81–142.06 kJ/mol, and 133.26 kJ/mol, respectively. The thermodynamic parameters were determined but only by FWO and KAS. It is interesting to note that the E_a values found were as low as 133.26 kJ/mol, while enthalpy was 128 kJ/mol [72]. Other studies of microalgae mention that the characteristics and kinetics of this biomass during pyrolysis are essential for designing pyrolyzers and optimizing processes; indeed, the pyrolysis kinetics of this kind of biomass has become a topic of growing interest among researchers. A TGA analysis of the microalga, *Dunaliella tertiolecta*, applied the KAS and FWO methods to determine E_a values between 131.7 and 152.7 kJ/mol by KAS and 134.4–152.9 kJ/mol by FWO. E_a values of 43.7–67.6 kJ/mol and 41.2–63.7 kJ/mol have been reported for *Chlorella vulgaris* by the FWO and KAS methods, respectively. The Freeman–Carroll method was used in an analysis of the microalga, *Chlorella Spp*, obtaining E_a values between 71.3 and 79.2 kJ/mol [73]. The variation of hydrogen in different types of microalgae analyzed ranged from 5.37% for *Dunaliella tertiolecta* [74] to 7.7% for *Nannochloropsis gaditana* [75].

Another study included *Chlorella vulgaris* with the microalgae species *Dunaliella salina* and *Haematococcus pluvialis*, common sources of lignocellulosic biomass in China. It used Friedman's method to evaluate E_a , which was considered when the value of the degree of advance was less than 0.75. This required six heating speeds (5, 10, 20, 30, 40, 50 °C/min). That study also compared a kinetic model to the experimental model to demonstrate that thermal degradation was governed by a complex process, which was further proven by a differential thermogravimetric analysis (DTG) that observed two main exothermic peaks which corresponded to carbohydrates and lipids. E_a values varied from over 100 kJ/mol to below 300 kJ/mol for this marine biomass. Hydrogen content averaged 7% [76].

Another study evaluated the potential bioenergy of the aquatic plant *Wolffia arrhizal* using pyrolysis. The biomass was gathered from a pond that receives waste water from a textile factory. Thermal degradation was performed at three heating speeds (10, 30, 50 °C/min) in an inert nitrogen atmosphere (100 mL/min). The data obtained were subjected to the KAS and FWO models to obtain E_a values of 168.35 and 170.37 kJ/mol, respectively, and similar enthalpy values of 163.29 and 165.31 kJ/mol. The elemental composition

analysis showed a hydrogen content of 6.36%. Gas chromatography/mass spectrometry (GC/MS) analysis revealed diverse compounds that contained toluene, benzene, and acetylene and presented an HHV comparable to that of diesel fuel (44.8 MJ/kg) and gasoline (47.3 MJ/kg). That study demonstrated that this biomass can be used to produce both energy and chemical products through a process that is profitable and ecological [77].

A similar study focused on water lentils of the subfamily *Lemmaoideae*, collected in Waterloo (Ontario, Canada). This plant grows very quickly, with reports that it doubles its mass in just two or three days. Annually, it can generate as much as 55 tons of biomass per hectare [78]. Recent studies of ethanol and biogas production have found yields as much as 50% greater than corn [79]. In efforts to achieve greater precision and control in pyrolysis processes and, therefore, in kinetic parameters, such as E_a , the KAS and FWO methods were complemented by DAEM. That study used three heating speeds (10, 20, 30 °C/min) in a temperature range of 25–802 °C in a nitrogen atmosphere at a flow of 60 mL/min. The Friedman, KAS, FWO, and DAEM models were used to determine the kinetic parameters. Similar to other biomasses, TGA analysis showed that the degradation of the polymers followed the sequence hemicellulose-cellulose-lignin due to their chemical properties. The variation in E_a by Friedman, KAS, and FWO was very low, as values of 160–300 kJ/mol were reported throughout the range of the degree of advance. By DAEM, this value rose from 110 to 360 kJ/mol, demonstrating that predictions of the results of pyrolysis for water lentils using this model are quite accurate [80].

3.4.2. Kinetics of Dried Fruits

Yet another study used tropical almonds from Modakeke (Osun state, Nigeria) based on TGA data at heating speeds of 10, 15, and 30 °C/min in an inert atmosphere. Kinetic analysis was by FWO, KAS, and DAEM. The general approximate value for E_a was 130 kJ/mol, the frequency factor had orders of magnitude in the range of 10^{11} to 10^{12} , while R^2 was greater than 0.99. The authors concluded that a pyrolytic reactor fueled by residue from tropical almonds from Nigeria could significantly reduce contaminating emissions, such as CO₂. The HHV of 25.07 MJ/kg is another advantage of this biomass [81].

Nutshell has also been studied for energy production. For example, the degradation kinetics of betel nut shell from India have been analyzed using pyrolysis and the KAS, FWO, Friedman, CR, and DAEM models. That study used five heating speeds (5, 10, 15, 20, 25 °C/min) in an inert nitrogen atmosphere at a flow of 50 mL/min. To determine the kinetic parameters, the authors considered a conversion range of 0.1–0.7. Results showed E_a values of 171.24, 179.47, 184.61, and 160.45 kJ/mol for the KAS, FWO, Friedman, and DAEM models, respectively. R^2 was above 0.9, in some cases reaching 0.99 ($\alpha = 0.7$). For the CR model, which operates at only one heating speed (10 °C/min in this study), E_a was 63.41 kJ/mol with a $n = 1$. This value was lower than in the other models (KAS, FWO, Friedman, DAEM) because the CR equation focuses only on the devolatilization stage and char combustion, while the other four methods reveal the distribution of E_a and even the A of the entire combustion process [51,82].

A residue that has drawn attention in Mexico derives from peanut production, a plant of the family *Fabaceae*. Average annual peanut production there is 115,000 tons, obtained from a surface area of approximately 60,000 hectares. This production generates almost 30,000 tons of peanut shell annually, representing 30% of the crop's weight. To determine the potential for exploiting this residue, a thermal valorization study was carried out using pyrolysis in a nitrogen atmosphere at a flow of 100 mL/min, three heating speeds (5, 10, 50 °C/min), and a temperature range of 25–1000 °C. As a function of the degradation of the primary components in the second and fourth stages of the TGA analysis (hemicellulose, cellulose, lignin) the average E_a values reported were 172, 209, and 200–300 kJ/mol, respectively, for the Kissinger, Friedman, and KAS models. R^2 values by Kissinger's method were above 0.99. That thermal process was found to be highly exothermic and defined by the first-order reaction, $f(\alpha) = 1 - \alpha$ [83].

4. Conclusions

This article presented a broad review of over 20 types of terrestrial and marine biomass that have been studied using diverse mathematical models to interpret their kinetics. Each case explored included the principal kinetic parameters— E_a , A , and n —of the thermal of pyrolysis process of diverse lignocellulosic and non-lignocellulosic materials, and some with low content of the primary components (hemicellulose, cellulose, lignin). The overview shows that these parameters were determined mainly by the Flynn–Wall–Ozawa and Kissinger–Akahira–Sunose iso-conversional and integral models, though other important models in this category were also applied: Popescu, Coats–Redfern, DAEM, and Vyazovkin, as well as Friedman’s model, which is iso-conversional and classified as a differential model, and Kissinger’s model, which is iso-conversional. In general, it can be considered that the best kinetic models are Flynn–Wall–Ozawa and Kissinger–Akahira–Sunose due to their greater applicability and similarity in results, although fitting models, such as Coats–Redfern and Vyazovkin, also provide very good results in kinetic studies in thermogravimetric processes of lignocellulosic biomass. In practical terms, the TGA analysis and the resulting kinetic parameters— E_a , A , and n —are of great importance in pyrolytic processes at an industrial level; they serve as an important support to determine ideal conditions in the process, such as temperatures, quantities, and concentrations of reagents with which a deeper analysis can be performed to scale up the results in the manufacture of equipment for biomass pyrolytic processes. The final conclusion is that applying kinetic models makes it possible to infer the thermal stability of biomass residues, when subjected to thermal processes, such as pyrolysis.

This article presented a broad review of over 20 types of terrestrial and marine biomass that have been studied using diverse mathematical models to interpret their kinetics. Each case explored included the principal kinetic parameters— E_a , A , and n —of the thermal of pyrolysis process of diverse lignocellulosic and non-lignocellulosic materials, and some with low content of the primary components (hemicellulose, cellulose, lignin). The overview shows that these parameters were determined mainly by the Flynn–Wall–Ozawa and Kissinger–Akahira–Sunose iso-conversional and integral models, though other important models in this category were also applied: Popescu, Coats–Redfern, DAEM, and Vyazovkin, as well as Friedman’s model, which is iso-conversional and classified as a differential model, and Kissinger’s model, which is iso-conversional. In general, it can be considered that the best kinetic models are Flynn–Wall–Ozawa and Kissinger–Akahira–Sunose due to their greater applicability and similarity in results, although fitting models, such as Coats–Redfern and Vyazovkin, also provide very good results in kinetic studies in thermogravimetric processes of lignocellulosic biomass. In practical terms, the TGA analysis and the resulting kinetic parameters— E_a , A , and n —are of great importance in pyrolytic processes at an industrial level; they serve as an important support to determine ideal conditions in the process, such as temperatures, quantities, and concentrations of reagents with which a deeper analysis can be performed to scale up the results in the manufacture of equipment for biomass pyrolytic processes. The final conclusion is that applying kinetic models makes it possible to infer the thermal stability of biomass residues, when subjected to thermal processes, such as pyrolysis.

Author Contributions: Writing—original draft preparation, J.J.A.F., J.G.R.Q., J.V.A.V., M.L.Á.R., R.A.Z. and L.B.L.S.; conceptualization, J.J.A.F., J.V.A.V., M.L.Á.R., R.A.Z. and L.B.L.S.; data curation, J.J.A.F., J.G.R.Q., L.F.P.I., J.V.A.V., M.L.Á.R., L.B.L.S. and F.M.M.; formal analysis, J.J.A.F., J.V.A.V. and M.L.Á.R.; investigation, J.J.A.F., J.G.R.Q., L.F.P.I., J.V.A.V., M.L.Á.R., L.B.L.S., R.A.Z. and F.M.M.; methodology, J.J.A.F., J.G.R.Q., J.V.A.V. and M.L.Á.R.; supervision, L.F.P.I., J.V.A.V., R.A.Z., L.B.L.S. and F.M.M. All authors have read and agreed to the published version of the manuscript.

Funding: This research received no external funding.

Institutional Review Board Statement: Not applicable.

Informed Consent Statement: Not applicable.

Data Availability Statement: Not applicable.

Acknowledgments: The authors thank the Faculty of Engineering in Wood Technology of the Universidad Michoacana de San Nicolás de Hidalgo for their support in the development of this research.

Conflicts of Interest: The authors declare no conflict of interest.

References

1. Burke, M.J.; Stephens, J.C. Energy democracy: Goals and policy instruments for sociotechnical transitions. *Energy Res. Soc. Sci.* **2017**, *33*, 35–48. [[CrossRef](#)]
2. York, R.; Bell, S.E. Energy transitions or additions?: Why a transition from fossil fuels requires more than the growth of renewable energy. *Energy Res. Soc. Sci.* **2019**, *51*, 40–43. [[CrossRef](#)]
3. Morales-Máximo, M.; Castro-Sánchez, F.J.; Rutiaga-Quiñones, J.G. Estudio socioeconómico para la evaluación de biocombustibles sólidos: Eficiencia energética y alterna en la comunidad de San Francisco Pichátaro, Michoacán, México. *Int. Energy Conf. IEC* **2019**, *2*, 577–582.
4. Huang, J.; Zhang, J.; Liu, J.; Xie, W.; Kuo, J.; Chang, K.; BuyuKada, M.; Evrendilek, F.; Sun, S.J. Thermal conversion behaviors and products of spent mushroom substrate in CO₂ and N₂ atmospheres: Kinetic, thermodynamic, TG and Py-GC/MS analyses. *Anal. Appl. Pyrol.* **2019**, *139*, 177–186. [[CrossRef](#)]
5. Languer, M.P.; Batistella, L.; Alves, J.L.F.; Da Silva, J.C.G.; Filho, V.F.D.S.; Di Domenico, M.; Moreira, R.D.F.P.M.; José, H.J. Insights into pyrolysis characteristics of Brazilian high-ash sewage sludges using thermogravimetric analysis and bench-scale experiments with GC-MS to evaluate their bioenergy potential. *Biomass Bioenergy* **2020**, *138*, 105614. [[CrossRef](#)]
6. Parthasarathy, P.; Narayanan, K.S. Hydrogen production from steam gasification of biomass: Influence of process parameters on hydrogen yield—A review. *Renew. Energy* **2014**, *66*, 570–579. [[CrossRef](#)]
7. Demirbas, A. Hydrogen-rich gas from fruit shale via supercritical water extraction. *Int. J. Hydrogen Energy* **2004**, *29*, 1237–1243. [[CrossRef](#)]
8. Shahabuddin, M.; Krishna, B.B.; Bhaskar, T.; Perkins, G. Advances in the thermo-chemical production of hydrogen from biomass and residual wastes: Summary of recent techno-economic analyses. *Bioresour. Technol.* **2020**, *299*, 122557. [[CrossRef](#)]
9. da Silva, J.C.G.; Andersen, S.L.F.; Costa, R.L.; Moreira, R.D.F.P.M.; José, H.J. Bioenergetic potential of Ponkan peel waste (*Citrus reticulata*) pyrolysis by kinetic modelling and product characterization. *Biomass Bioenergy* **2019**, *131*, 105401. [[CrossRef](#)]
10. Tahir, M.H.; Zhao, Z.; Ren, J.; Rasool, T.; Naqvi, S.R. Thermo-kinetics and gaseous product analysis of banana peel pyrolysis for its bioenergy potential. *Biomass Bioenergy* **2019**, *122*, 193–201. [[CrossRef](#)]
11. Ahmad, M.S.; Mehmood, M.A.; Al Ayed, O.S.; Ye, G.; Luo, H.; Ibrahim, M.; Rashid, U.; Nehdi, I.A.; Qadir, G. Kinetic analyses and pyrolytic behavior of Para grass (*Urochloa mutica*) for its bioenergy potential. *Bioresour. Technol.* **2017**, *224*, 708–713. [[CrossRef](#)] [[PubMed](#)]
12. Correa-Méndez, F.; Carrillo-Parra, A.; Rutiaga-Quiñones, J.G.; Márquez-Montesino, F.; González-Rodríguez, H.; Jurado Ybarra, E.; Garza-Ocañas, F. Distribución granulométrica en subproductos de aserrío para su posible uso en pellets y briquetas. *Rev. Mex. Cienc. For.* **2014**, *5*, 52–63.
13. Núñez-Retana, V.D.; Wehenkel, C.; Vega-Nieva, D.J.; García-Quezada, J.; Carrillo-Parra, A. The bioenergetic potential of four oak species from northeastern Mexico. *Forests* **2019**, *10*, 869. [[CrossRef](#)]
14. Beltrán, L.R.; Alexandri, R.R.; Herrera, J.R.; Ojeda, O.G. Balance Nacional de Energía. *Secr. Energía Subsecr. Planeación Y Transic. Energética* **2018**, *15*.
15. Hernández-Escobedo, Q.; Perea-Moreno, A.J.; Manzano-Agugliaro, F. Wind energy research in Mexico. *Renew. Energy* **2018**, *123*, 719–729. [[CrossRef](#)]
16. Van Dael, M.; Lizin, S.; Swinnen, G.; Van Passel, S. Young people's acceptance of bioenergy and the influence of attitude strength on information provision. *Renew. Energy* **2017**, *107*, 417–430. [[CrossRef](#)]
17. Zhang, Z.; He, C.; Sun, T.; Zhang, Z.; Song, K.; Wu, Q.; Zhang, Q. Thermo-physical properties of pretreated agricultural residues for bio-hydrogen production using thermo-gravimetric analysis. *Int. J. Hydrogen Energy* **2016**, *41*, 5234–5242. [[CrossRef](#)]
18. Saqib, N.U.; Baroutian, S.; Sarmah, A.K. Physicochemical, structural and combustion characterization of food waste hydrochar obtained by hydrothermal carbonization. *Bioresour. Technol.* **2018**, *266*, 357–363. [[CrossRef](#)] [[PubMed](#)]
19. Hu, M.; Wang, X.; Chen, J.; Yang, P.; Liu, C.; Xiao, B.; Guo, D. Kinetic study and syngas production from pyrolysis of forestry waste. *Energy Convers. Manag.* **2017**, *135*, 453–462. [[CrossRef](#)]
20. Tang, Y.; Ma, X.; Wang, Z.; Wu, Z.; Yu, Q. A study of the thermal degradation of six typical municipal waste components in CO₂ and N₂ atmospheres using TGA-FTIR. *Thermochim. Acta* **2017**, *657*, 12–19. [[CrossRef](#)]
21. Zhang, Z.P. Study on the Technology of Ultramicro Pretreatment by Straw Biomass and Feasibility Study of Hydrogen Production. Master's Thesis, Henan Agricultural University, Zhengzhou, China, 2012.
22. Cai, J.; Xu, D.; Dong, Z.; Yu, X.; Yang, Y.; Banks, S.W.; Bridgwater, A.V. Processing thermogravimetric analysis data for isoconversional kinetic analysis of lignocellulosic biomass pyrolysis: Case study of corn stalk. *Renew. Sustain. Energy Rev.* **2018**, *82*, 2705–2715. [[CrossRef](#)]

23. Alvarado Flores, J.J.; Rutiaga Quiñones, J.G.; Ávalos Rodríguez, M.L.; Alcaraz Vera, J.V.; Espino Valencia, J.; Guevara Martínez, S.J.; Márquez Montesino, F.; Alfaro Rosas, A. Thermal degradation kinetics and FT-IR analysis on the pyrolysis of *Pinus pseudostrobus*, *Pinus leiophylla* and *Pinus montezumae* as forest waste in Western Mexico. *Energies* **2020**, *13*, 969. [CrossRef]
24. Wang, S.; Dai, G.; Yang, H.; Luo, Z. Lignocellulosic biomass pyrolysis mechanism: A state-of-the-art review. *Prog. Energy Combust.* **2017**, *62*, 33–86. [CrossRef]
25. Zhang, J.; Liu, J.; Evrendilek, F.; Zhang, X.; Buyukada, M. TG-FTIR and Py-GC/MS analyses of pyrolysis behaviors and products of cattle manure in CO₂ and N₂ atmospheres: Kinetic, thermodynamic, and machine-learning models. *Energy Convers. Manag.* **2019**, *195*, 346–359. [CrossRef]
26. Wen, S.; Yan, Y.; Liu, J.; Buyukada, M.; Evrendilek, F. Pyrolysis performance, kinetic, thermodynamic, product and joint optimization analyses of incense sticks in N₂ and CO₂ atmospheres. *Renew. Energy* **2019**, *141*, 814–827. [CrossRef]
27. Cai, J.; He, Y.; Yu, X.; Banks, S.W.; Yang, Y.; Zhang, X.; Liu, R.; Bridgwater, A.V. Review of physicochemical properties and analytical characterization of lignocellulosic biomass. *Renew. Sustain. Energy Rev.* **2017**, *76*, 309–322. [CrossRef]
28. Xu, L.; Zhou, J.; Ni, J.; Li, Y.; Long, Y.; Huang, R. Investigating the pyrolysis kinetics of *Pinus sylvestris* using thermogravimetric analysis. *BioResources* **2020**, *15*, 5577–5592. [CrossRef]
29. Cui, B.; Chen, Z.; Guo, D.; Liu, Y. Investigations on the pyrolysis of microalgal-bacterial granular sludge: Products, kinetics, and potential mechanisms. *Bioresour. Technol.* **2022**, *349*, 126328. [CrossRef] [PubMed]
30. Flores, J.J.A.; Vera, J.V.A.; Rodríguez, M.L.Á.; Quiñones, J.G.R.; Valencia, J.E.; Martínez, S.J.G.; Tututi, E.R.; Zarraga, R.A. Kinetic, thermodynamic, FT-IR, and primary constitution analysis of *Sargassum* spp from Mexico: Potential for hydrogen generation. *Int. J. Hydrogen Energy* **2022**, *47*, 30107–30127. [CrossRef]
31. Marques, M.B.; Araujo, B.C.; Fernandes, C.; Yoshida, M.I.; Mussel, W.N.; Sebastião, R.C. Kinetics of lumefantrine thermal decomposition employing isoconversional models and artificial neural network. *J. Brazil Chem. Soc.* **2020**, *31*, 512–522. [CrossRef]
32. Laougé, Z.B.; Merdun, H. Pyrolysis and combustion kinetics of *Sida cordifolia* L. using thermogravimetric analysis. *Bioresour. Technol.* **2020**, *299*, 122602. [CrossRef]
33. Rony, A.H.; Kong, L.; Lu, W.; Dejam, M.; Adidharma, H.; Gasem, K.A.; Zheng, Y.; Norton, U.; Fan, M. Kinetics, thermodynamics, and physical characterization of corn stover (*Zea mays*) for solar biomass pyrolysis potential analysis. *Bioresour. Technol.* **2019**, *284*, 466–473. [CrossRef]
34. India Maize Summit. Aspevid = 21821 (FICCI). 2014. Available online: <http://www.ficci.in/past-event-page> (accessed on 18 April 2022).
35. Gupta, G.K.; Mondal, M.K. Kinetics and thermodynamic analysis of maize cob pyrolysis for its bioenergy potential using thermogravimetric analyzer. *J. Therm. Anal. Calorim.* **2019**, *137*, 1431–1441. [CrossRef]
36. Shi, S.; Zhou, X.; Chen, W.; Wang, X.; Nguyen, T.; Chen, M. Thermal and kinetic behaviors of fallen leaves and waste tires using thermogravimetric analysis. *BioResources* **2017**, *12*, 4707–4721. [CrossRef]
37. Aslan, D.I.; Parthasarathy, P.; Goldfarb, J.L.; Ceylan, S. Pyrolysis reaction models of waste tires: Application of Master-Plots method for energy conversion via devolatilization. *Waste Manag.* **2017**, *68*, 405–411. [CrossRef] [PubMed]
38. Zou, H.; Evrendilek, F.; Liu, J.; Buyukada, M. Combustion behaviors of pileus and stipe parts of *Lentinus edodes* using thermogravimetric-mass spectrometry and Fourier transform infrared spectroscopy analyses: Thermal conversion, kinetic, thermodynamic, gas emission and optimization analyses. *Bioresour. Technol.* **2019**, *288*, 121481. [CrossRef]
39. Ding, Y.; Zhang, Y.; Zhang, J.; Zhou, R.; Ren, Z.; Guo, H. Kinetic parameters estimation of pinus sylvestris pyrolysis by Kissinger-Kai method coupled with Particle Swarm Optimization and global sensitivity analysis. *Bioresour. Technol.* **2019**, *293*, 122079. [CrossRef]
40. Mureddu, M.; Dessì, F.; Orsini, A.; Ferrara, F.; Pettinau, A. Air-and oxygen-blown characterization of coal and biomass by thermogravimetric analysis. *Fuel* **2018**, *212*, 626–637. [CrossRef]
41. Mehmood, M.A.; Ye, G.; Luo, H.; Liu, C.; Malik, S.; Afzal, I.; Xu, J.; Ahmad, M.S. Pyrolysis and kinetic analyses of Camel grass (*Cymbopogon schoenanthus*) for bioenergy. *Bioresour. Technol.* **2017**, *228*, 18–24. [CrossRef]
42. Müsellim, E.; Tahir, M.H.; Ahmad, M.S.; Ceylan, S. Thermokinetic and TG/DSC-FTIR study of pea waste biomass pyrolysis. *Appl. Therm. Eng.* **2018**, *137*, 54–61. [CrossRef]
43. Song, Y.; Liu, J.; Evrendilek, F.; Kuo, J.; Buyukada, M. Combustion behaviors of *Pteris vittata* using thermogravimetric, kinetic, emission and optimization analyses. *J. Clean. Prod.* **2019**, *237*, 117772. [CrossRef]
44. Gogoi, M.; Konwar, K.; Bhuyan, N.; Borah, R.C.; Kalita, A.C.; Nath, H.P.; Saikia, N. Assessments of pyrolysis kinetics and mechanisms of biomass residues using thermogravimetry. *Bioresour. Technol. Rep.* **2018**, *4*, 40–49. [CrossRef]
45. Gupta, A.; Thengane, S.K.; Mahajani, S. Kinetics of pyrolysis and gasification of cotton stalk in the central parts of India. *Fuel* **2020**, *263*, 116752. [CrossRef]
46. Hu, J.; Yan, Y.; Evrendilek, F.; Buyukada, M.; Liu, J. Combustion behaviors of three bamboo residues: Gas emission, kinetic, reaction mechanism and optimization patterns. *J. Clean. Prod.* **2019**, *235*, 549–561. [CrossRef]
47. Liang, F.; Wang, R.; Hongzhong, X.; Yang, X.; Zhang, T.; Hu, W.; Mi, B.; Liu, Z. Investigating pyrolysis characteristics of moso bamboo through TG-FTIR and Py-GC/MS. *Bioresour. Technol.* **2018**, *256*, 53–60. [CrossRef]
48. Ding, Y.; Ezekoye, O.A.; Lu, S.; Wang, C.; Zhou, R. Comparative pyrolysis behaviors and reaction mechanisms of hardwood and softwood. *Energy Convers. Manag.* **2017**, *132*, 102–109. [CrossRef]

49. Xu, X.; Pan, R.; Chen, R.; Zhang, D. Comparative pyrolysis characteristics and kinetics of typical hardwood in inert and oxygenous atmosphere. *Appl. Biochem. Biotech.* **2020**, *190*, 90–112. [[CrossRef](#)] [[PubMed](#)]
50. Liu, H.; Wang, C.; Zhao, W.; Yang, S.; Hou, X. Pyrolysis characteristics and kinetic modeling of *Artemisia apiacea* by thermogravimetric analysis. *J. Therm. Anal. Calorim.* **2018**, *131*, 1783–1792. [[CrossRef](#)]
51. Fernandez, A.; Mazza, G.; Rodriguez, R. Thermal decomposition under oxidative atmosphere of lignocellulosic wastes: Different kinetic methods application. *J. Environ. Chem. Eng.* **2018**, *6*, 404–415. [[CrossRef](#)]
52. Luo, L.; Guo, X.; Zhang, Z.; Chai, M.; Rahman, M.M.; Zhang, X.; Cai, J. Insight into pyrolysis kinetics of lignocellulosic biomass: Isoconversional kinetic analysis by the modified friedman method. *Energy Fuels* **2020**, *34*, 4874–4881. [[CrossRef](#)]
53. Ye, G.; Luo, H.; Ren, Z.; Ahmad, M.S.; Liu, C.G.; Tawab, A.; Ghafari, A.B.; Omar, U.; Gull, M.; Mehmood, M.A. Evaluating the bioenergy potential of Chinese Liquor-industry waste through pyrolysis, thermogravimetric, kinetics and evolved gas analyses. *Energy Convers. Manag.* **2018**, *163*, 13–21. [[CrossRef](#)]
54. Rahib, Y.; Sarh, B.; Bostyn, S.; Bonnamy, S.; Boushaki, T.; Chaoufi, J. Non-isothermal kinetic analysis of the combustion of argan shell biomass. *Mater. Today Proc.* **2020**, *24*, 11–16. [[CrossRef](#)]
55. Arenas, C.N.; Navarro, M.V.; Martínez, J.D. Pyrolysis kinetics of biomass wastes using isoconversional methods and the distributed activation energy model. *Bioresour. Technol.* **2019**, *288*, 121485. [[CrossRef](#)] [[PubMed](#)]
56. Loy, A.C.M.; Yusup, S.; Chin, B.L.F.; Gan, D.K.W.; Shahbaz, M.; Acda, M.N.; Unrean, P.; Rianawati, E. Comparative study of in-situ catalytic pyrolysis of rice husk for syngas production: Kinetics modelling and product gas analysis. *J. Clean. Prod.* **2018**, *197*, 1231–1243. [[CrossRef](#)]
57. Loy, A.C.M.; Gan, D.K.W.; Yusup, S.; Chin, B.L.F.; Lam, M.K.; Shahbaz, M.; Unrean, P.; Acda, M.N.; Rianawati, E. Thermogravimetric kinetic modelling of in-situ catalytic pyrolytic conversion of rice husk to bioenergy using rice hull ash catalyst. *Bioresour. Technol.* **2018**, *261*, 213–222. [[CrossRef](#)]
58. Ashraf, A.; Sattar, H.; Munir, S. A comparative applicability study of model-fitting and model-free kinetic analysis approaches to non-isothermal pyrolysis of coal and agricultural residues. *Fuel* **2019**, *240*, 326–333. [[CrossRef](#)]
59. Fernandes, E.R.K.; Marangoni, C.; Souza, O.; Sellin, N. Thermochemical characterization of banana leaves as a potential energy source. *Energy Convers. Manag.* **2013**, *75*, 603–608. [[CrossRef](#)]
60. Cheng, Q.; Jiang, M.; Chen, Z.; Wang, X.; Xiao, B. Pyrolysis and kinetic behavior of banana stem using thermogravimetric analysis. *Energy Sources Part A* **2016**, *38*, 3383–3390. [[CrossRef](#)]
61. Singh, R.K.; Pandey, D.; Patil, T.; Sawarkar, A.N. Pyrolysis of banana leaves biomass: Physico-chemical characterization, thermal degradation behavior, kinetic and thermodynamic analyses. *Bioresour. Technol.* **2020**, *310*, 123464. [[CrossRef](#)] [[PubMed](#)]
62. Wei, R.; Huang, S.; Wang, Z.; Wang, X.; Ding, C.; Yuen, R.; Wang, J. Thermal behavior of nitrocellulose with different aging periods. *J. Therm. Anal. Calorim.* **2019**, *136*, 651–660. [[CrossRef](#)]
63. Wei, R.; Huang, S.; Wang, Z.; Yuen, R.; Wang, J. Evaluation of the critical safety temperature of nitrocellulose in different forms. *J. Loss Prevent. Proc.* **2018**, *56*, 289–299. [[CrossRef](#)]
64. Wei, R.; Huang, S.; Wang, Z.; Wang, C.; Zhou, T.; He, J.; Yuen, R.; Wang, J. Effect of plasticizer dibutyl phthalate on the thermal decomposition of nitrocellulose. *J. Therm. Anal. Calorim.* **2018**, *134*, 953–969. [[CrossRef](#)]
65. Alhumade, H.; da Silva, J.C.G.; Ahmad, M.S.; Çakman, G.; Yıldız, A.; Ceylan, S.; Elkamel, A. Investigation of pyrolysis kinetics and thermal behavior of Invasive Reed Canary (*Phalaris arundinacea*) for bioenergy potential. *J. Anal. Appl. Pyrol.* **2019**, *140*, 385–392. [[CrossRef](#)]
66. Matali, S.; Abd Rahman, N.; Idris, S.S.; Yaacob, N. Dynamic Model-Free and Model-Fitting Kinetic Analysis during Torrefaction of Oil Palm Frond Pellets. *Bull. Chem. Reaction Eng. Catal.* **2020**, *15*, 253–263. [[CrossRef](#)]
67. Kumar, M.; Upadhyay, S.N.; Mishra, P.K. Effect of Montmorillonite clay on pyrolysis of paper mill waste. *Bioresour. Technol.* **2020**, *307*, 123161. [[CrossRef](#)] [[PubMed](#)]
68. Fang, S.; Lin, Y.; Lin, Y.; Chen, S.; Shen, X.; Zhong, T.; Ding, L.; Ma, X. Influence of ultrasonic pretreatment on the co-pyrolysis characteristics and kinetic parameters of municipal solid waste and paper mill sludge. *Energy* **2020**, *190*, 116310. [[CrossRef](#)]
69. Mishra, R.K.; Mohanty, K. Kinetic analysis and pyrolysis behaviour of waste biomass towards its bioenergy potential. *Bioresour. Technol.* **2020**, *311*, 123480. [[CrossRef](#)] [[PubMed](#)]
70. Fan, S.; Tang, J.; Wang, Y.; Li, H.; Zhang, H.; Tang, J.; Wang, Z.; Li, X. Biochar prepared from co-pyrolysis of municipal sewage sludge and tea waste for the adsorption of methylene blue from aqueous solutions: Kinetics, isotherm, thermodynamic and mechanism. *J. Mol. Liq.* **2016**, *220*, 432–441. [[CrossRef](#)]
71. Cai, H.; Liu, J.; Xie, W.; Kuo, J.; Buyukada, M.; Evrendilek, F. Pyrolytic kinetics, reaction mechanisms and products of waste tea via TG-FTIR and Py-GC/MS. *Energy Convers. Manag.* **2019**, *184*, 436–447. [[CrossRef](#)]
72. Fong, M.J.B.; Loy, A.C.M.; Chin, B.L.F.; Lam, M.K.; Yusup, S.; Jawad, Z.A. Catalytic pyrolysis of *Chlorella vulgaris*: Kinetic and thermodynamic analysis. *Bioresour. Technol.* **2019**, *289*, 121689. [[CrossRef](#)]
73. Bach, Q.V.; Chen, W.H. Pyrolysis characteristics and kinetics of microalgae via thermogravimetric analysis (TGA): A state-of-the-art review. *Bioresour. Technol.* **2017**, *246*, 88–100. [[CrossRef](#)] [[PubMed](#)]
74. Shuping, Z.; Yulong, W.; Mingde, Y.; Chun, L.; Junmao, T. Pyrolysis characteristics and kinetics of the marine microalgae *Dunaliella tertiolecta* using thermogravimetric analyzer. *Bioresour. Technol.* **2010**, *101*, 359–365. [[CrossRef](#)] [[PubMed](#)]
75. López-González, D.; Fernandez-Lopez, M.; Valverde, J.L.; Sanchez-Silva, L. Pyrolysis of three different types of microalgae: Kinetic and evolved gas analysis. *Energy* **2014**, *73*, 33–43. [[CrossRef](#)]

76. Vasudev, V.; Ku, X.; Lin, J. Kinetic study and pyrolysis characteristics of algal and lignocellulosic biomasses. *Bioresour. Technol.* **2019**, *288*, 121496. [[CrossRef](#)] [[PubMed](#)]
77. Ahmad, M.S.; Mehmood, M.A.; Liu, C.G.; Tawab, A.; Bai, F.W.; Sakdaronnarong, C.; Xu, J.; Rahimuddin, S.A.; Gull, M. Bioenergy potential of *Wolffia arrhiza* appraised through pyrolysis, kinetics, thermodynamics parameters and TG-FTIR-MS study of the evolved gases. *Bioresour. Technol.* **2018**, *253*, 297–303. [[CrossRef](#)]
78. Liu, Y.; Chen, X.; Wang, X.; Fang, Y.; Zhang, Y.; Huang, M.; Zhao, H. The influence of different plant hormones on biomass and starch accumulation of duckweed: A renewable feedstock for bioethanol production. *Renew. Energy* **2019**, *138*, 659–665. [[CrossRef](#)]
79. Yadav, D.; Barbora, L.; Bora, D.; Mitra, S.; Rangan, L.; Mahanta, P. An assessment of duckweed as a potential lignocellulosic feedstock for biogas production. *Int. Biodeter. Biodegr.* **2017**, *119*, 253–259. [[CrossRef](#)]
80. Liu, H.; Ahmad, M.S.; Alhumade, H.; Elkamel, A.; Sammak, S.; Shen, B. A hybrid kinetic and optimization approach for biomass pyrolysis: The hybrid scheme of the isoconversional methods, DAEM, and a parallel-reaction mechanism. *Energy Convers. Manag.* **2020**, *208*, 112531. [[CrossRef](#)]
81. Olatunji, O.O.; Akinlabi, S.; Madushele, N.; Adedeji, P.A.; Ndolomingo, M.J.; Meshack, T. Blended tropical almond residue for fuel production: Characteristics, energy benefits, and emission reduction potential. *J. Clean. Prod.* **2020**, *267*, 122013. [[CrossRef](#)]
82. Mishra, R.K.; Mohanty, K. Pyrolysis kinetics and thermal behavior of waste sawdust biomass using thermogravimetric analysis. *Bioresour. Technol.* **2018**, *251*, 63–74. [[CrossRef](#)]
83. Torres-García, E.; Ramírez-Verduzco, L.F.; Aburto, J. Pyrolytic degradation of peanut shell: Activation energy dependence on the conversion. *Waste Manag.* **2020**, *106*, 203–212. [[CrossRef](#)] [[PubMed](#)]